Available online at www.sciencedirect.com
SCIENCE DIRECT®
Solid-State Electronics 47 (2003) 2231–2235
SOLID-STATE ELECTRONICS
www.elsevier.com/locate/sse

Ferromagnetism in Co- and Mn-doped ZnO

N.A. Theodoropoulou [a], A.F. Hebard [a], D.P. Norton [b,*], J.D. Budai [c], L.A. Boatner [c], J.S. Lee [d], Z.G. Khim [d], Y.D. Park [d], M.E. Overberg [b], S.J. Pearton [b], R.G. Wilson [e]

[a] *Department of Physics, University of Florida, Gainesville, FL 32611, USA*
[b] *Department of Materials Science and Engineering, University of Florida, Gainesville, FL 32611, USA*
[c] *Oak Ridge National Laboratories, Oak Ridge, TN 37831, USA*
[d] *School of Physics, Seoul National University, Seoul 151-747, South Korea*
[e] *Consultant, Stevenson Ranch, CA 91381, USA*

Received 21 August 2002; received in revised form 21 September 2002; accepted 6 December 2002

Abstract

Bulk single crystals of Sn-doped ZnO were implanted with Co or Mn at doses designed to produce transition metal concentrations of 3–5 at.% in the near-surface (~2000 Å) region. The implantation was performed at ~350 °C to promote dynamic annealing of ion-induced damage. Following annealing at 700 °C, temperature-dependent magnetization measurements showed ordering temperatures of ~300 K for Co- and ~250 K for Mn-implanted ZnO. Clear hysteresis loops were obtained at these temperatures. The coercive fields were $\leqslant 100$ Oe for all measurement temperatures. X-ray diffraction showed no detectable second phases in the Mn-implanted material. One plausible origin for the ferromagnetism in this case is a carrier-induced mechanism. By sharp contrast, the Co-implanted material showed evidence for the presence of Co precipitates with hexagonal symmetry, which is the cause of the room temperature ferromagnetism. Our results are consistent with the stabilization of ferromagnetic states by electron doping in transition metal-doped ZnO predicted by Sato and Katayama–Yoshida [Jpn. J. Appl. Phys. 40 (2001) L334]. This work shows the excellent promise of Mn-doped ZnO for potential room temperature spintronic applications.

Keywords: Oxides; Ferromagnetic semiconductor; Zinc oxide; Implantation

1. Introduction

ZnO is a direct band gap semiconductor with $E_g = 3.35$ eV and a large exciton bonding energy (60 meV) relative to its III-N counterparts (125 meV) [1,2]. The room temperature Hall mobility in ZnO single crystals is on the order of 200 $cm^2\,v^{-1}\,s^{-1}$ [3]. ZnO normally has a hexagonal (wurtzite) crystal structure with $a = 3.25$ Å and $c = 5.12$ Å. Electron doping via defects originates from Zn interstitials in the ZnO lattice [3]. The intrinsic defect levels that lead to n-type doping lie approximately 0.05 eV below the conduction band. High electron carrier density can also be realized via group III substitutional doping. While n-type ZnO is easily realized via excess Zn or with Al, Ga or In doping, p-type doping has proven difficult to achieve. Minegishi et al. reported the growth of p-type ZnO by the simultaneous addition of NH_3 in hydrogen carrier gas with excess Zn [4]. However, the resistivity of these films was high with $\rho \sim 100\ \Omega$ cm, suggesting that the mobile hole concentration was very low. Work by Rouleau et al. [5] on N-doped ZnO films shows that N incorporation does not necessarily yield p-type behavior. In this case, nitrogen doping in epitaxial ZnO films was achieved using a RF nitrogen plasma source in conjunction with pulsed-laser

* Corresponding author. Tel.: +1-352-846-0525; fax: +1-352-846-1182.
E-mail address: dnort@mse.ufl.edu (D.P. Norton).

0038-1101/$ - see front matter
doi:10.1016/S0038-1101(03)00203-X

deposition. However, they showed no p-type behavior as determined by Hall measurements. Ab initio electronic band structure calculations for ZnO based on the local density approximation show that the Madelung energy decreases with n-type doping, consistent with experimental results for electron doping with Al, Ga or In [6]. With N doping for holes, the Madelung energy increases, with significant localization of the N states. The theory does predict that co-doping N with Ga to form an N–Ga–N complex can decrease the Madelung energy and delocalize the N states, thus facilitating hole doping. Using pulsed-laser deposition, Joseph et al. has reported p-type behavior in ZnO thin films prepared by co-doping Ga and N [7]. Electrically active N was achieved by passing N_2O gas through an electron cyclotron resonance plasma source. The authors reported low resistivity ($\rho = 2\,\Omega\,\text{cm}$, carrier density $\sim 4 \times 10^{19}\ \text{cm}^{-3}$) p-type ZnO co-doped with Ga and N in which the Ga concentration ranged from 0.1% to 5%. Unfortunately, these results have proven highly sensitive to processing conditions, and have been difficult to reproduce.

While there have been significant efforts focusing on nitrogen doping, almost no reported work exists for either As or P doping. However, p–n junction-like behavior was reported for n-type ZnO in which the surface was heavily doped with phosphorus [8]. Laser annealing of a zinc phosphide-coated ZnO single crystal surface achieved the doping. A related result was reported for epitaxial ZnO films on GaAs subjected to annealing [9]. In this case, a p-type layer was produced at the GaAs/ZnO interface. Both of these reports are promising, but present several unresolved issues related to the solid solubility of the dopant (ionic radii of As, P much larger than that for O) and possible secondary phase formation in the doped region.

ZnO is also promising for potential spintronic applications. Dietl et al. [10] predicted a Curie temperature of $\geqslant 300$ K for Mn-doped ZnO, while electron-doping of Fe, Co or Ni-doped ZnO was predicted to stabilize high Curie temperature ferromagnetism [11,12]. Carrier-induced ferromagnetism was predicted for the case of hole doping of ZnO(Mn) [13,14], while methods for improving p-type doping have also been suggested [15]. Numerous reports of the magnetic properties of transition metal-doped ZnO have appeared recently [1,16–20]. Veda et al. [20] reported Curie temperatures above 300 K for Co-doped ZnO, Jung et al. [19] a T_C of 45 K for Mn-doped ZnO and Wakano et al. [17] a T_C of $\sim$2 K for Ni-doped ZnO.

In this paper, we report on the magnetic properties of bulk, Sn-doped ZnO crystals implanted with Co or Mn. In both cases we observe magnetization up to at least 250 K, although in the case of the Co-implanted material the ferromagnetism appears to arise from the presence of Co precipitates. These results show the potential of Mn-doped ZnO for spintronic applications.

2. Experimental

Bulk single-crystals of ZnO doped with Sn to produce an electron concentration of $\sim 10^{18}\ \text{cm}^{-3}$ were directly implanted with 250 keV Mn^+ or Co^+ ions at doses of 3 or $5 \times 10^{16}\ \text{cm}^{-2}$ into the (1 1 0) growth face. The samples were held at $\sim$350 °C during the implantation step to avoid amorphization of the ZnO lattice. The projected range of the implanted ions is $\sim$2000 Å, producing an average transition metal concentration of $\sim$3 or 5 at.%. The samples were subsequently annealed at 700°C for 5 min under flowing N_2 gas to repair implant damage. The magnetic properties were examined using a Quantum Design SQUID magnetometer, while the formation of second phases was examined by high resolution X-ray diffraction (XRD).

3. Results and discussion

3.1. Co-implantation

Fig. 1 shows magnetization loops at 5 K (top) and 300 K (bottom) from samples implanted with the 3 at.% dose of Co. Hysteresis is observed at both temperatures (figure inset), with coercivities <300 Oe. Fig. 2 shows the temperature dependence of the magnetization from a 3 at.% Co-implanted sample. The magnetization does not show the expected Brillouin-like dependence on temperature, but is consistent with the disorder model of Bhatt and co-workers [21–25]. Their model takes into account the effects of positional disorder of the magnetic impurities, in which the carriers are allowed to hop only between the transition metal dopants. The interaction between the carriers and the magnetic ions is an antiferromagnetic Heisenberg exchange type. The shape of the M–T plot is a function of the wide distribution of exchange couplings because some transition metal atoms do not order until lower temperatures.

Fig. 3 shows magnetization loops at 5 K (top) and 300 K (bottom) from the 5 at.% Co-implanted samples. Note that hysteresis is still observed under these conditions, in contrast to the system $SrTiO_3$ where we observed a very strong decrease of magnetization at high transition metal doping concentrations [26]. X-ray diffraction of the samples showed the presence of weak, broad peaks along the normal at $d = 1.258$ A in the theta–2 theta scans, as shown in Fig. 4. This peak is near the value expected for hexagonal Co precipitates oriented in the (1 1 0) direction or possibly cubic Co(2 2 0).We believe it is the former, since in other oxides the Co structure is controlled by the substrate structure. It is clear that the Co precipitates would have a strong influence on the magnetic properties since Co has a Curie temperature of 1382 K. It is still possible

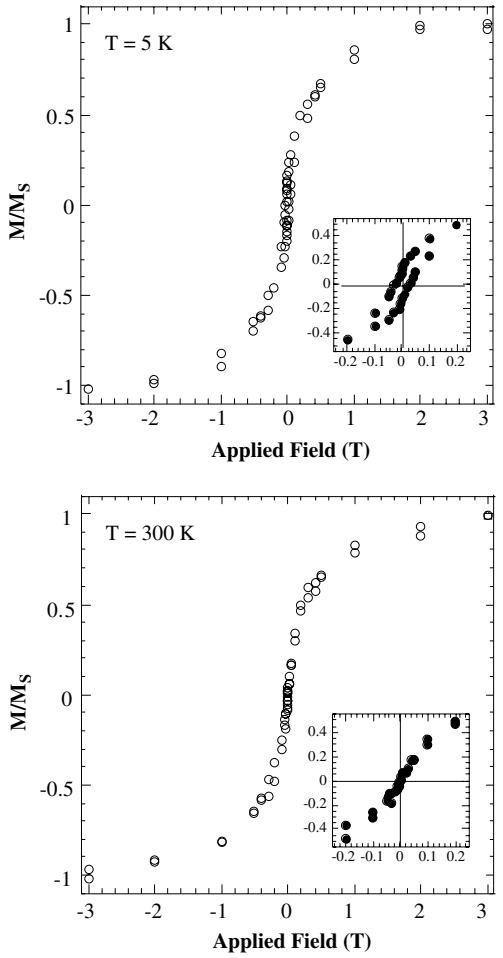

Fig. 1. Normalized magnetization loops at 5 K (top) and 300 K (bottom) for field applied parallel to the plane of a ZnO sample implanted with 3 at.% Co.

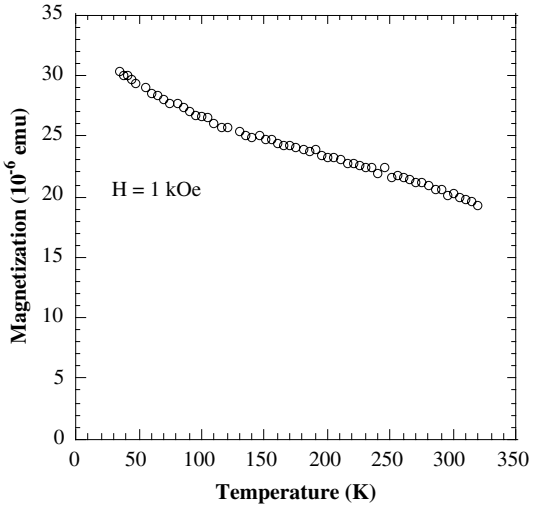

Fig. 2. Temperature dependence of magnetization at a field of 1000 G for a ZnO sample implanted with 3 at.% Co.

that some of the magnetism comes from a DMS host in addition to the Co precipitates. The final origin of the ferromagnetism in most transition-metal systems is not totally clear at this point and there are numerous models in the literature, none of which reproduce all of the experimental data, including the carrier-induced Zener ferromagnetism [10] and bound magnetic polarons [24].

3.2. Mn-implantation

Fig. 5 shows magnetization loops (top) and the temperature dependence of the difference in field-cooled and zero field-cooled magnetization from ZnO samples implanted with 3 at.% Mn. The magnetization resists to ~250 K, which is much higher than reported for Mn-doped epitaxial films, i.e. 45 K [19]. Note that once again the state of the M–T plot is consistent with the disorder model [20–25]. We expect that the crystal quality of our bulk ZnO is higher than the previously reported ZnMnO epi films and we are using lower Mn concentrations.

The Dietl et al. [10] near-field model considers the ferromagnetism to be mediated by delocalized or weakly localized holes in the p-type materials [10]. The magnetic Mn ion provides a localized spin and acts as an acceptor in most III–V semiconductors so that it can also provide holes. This treatment assumes that the Mn-doped III–V materials are charge transfer insulators and does not apply when d-shell electrons participate in charge transport. The spin–spin coupling is assumed to be a long-range interaction, allowing use of a mean-field approximation. The Curie temperature for a given material, Mn concentration and hole density is then determined by a competition between the ferromagnetic and antiferromagnetic interactions. The model takes into account the anisotropy of the carrier-mediated exchange interaction related with the spin–orbit coupling in the host material. The T_C proportional to the density of Mn ions and the hole density.In the absence of carriers, the magnetization $M_O(H)$ is dependent on the Brillouin function B_S according to [10]

$$M_O(H) = g\mu_B S N_O X_{eff} B_S\left[\frac{g\mu_S H}{K_B(T + T_{AF})}\right]$$

where g is the degeneracy factor, μ_B is the Bohr magneton, S is the localized spin state, N_O is the concentration of cation sites, $N_O X_{eff}$ is the effective spin concentration, k_B is Boltzmann's constant and the antiferromagnetic temperature T_{AF} describes the sum of the exchange interactions to the Curie–Weiss temperature. In the presence of carriers, the magnetization is represented as [10]

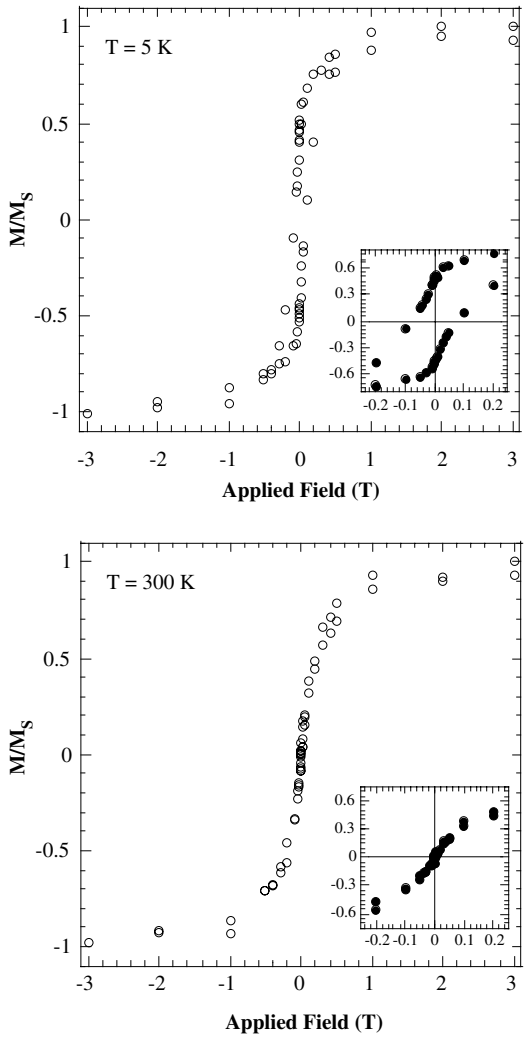

Fig. 3. Normalized magnetization loops at 5 K (top) and 300 K (bottom) for field applied parallel to the plane of a ZnO sample implanted with 5 at.% Co.

$$M = \mu_G \mu_B S N_O X_{eff} B_S[g\mu_B(-\Delta F_C[M]/\Delta M + H)/k_B(T + T_{AF})]$$

where $F_C[M]$ is the hole contribution to the free-energy functional F, which is dependent on the magnetization of the localized spin. From this relation, T_C can be expressed [10]

$$T_C = X_{eff} N_O S(S+1)\beta^2 A_F P_S(T_C)/12k_B - T_{AF}$$

where β is the p–d exchange integral, A_F is the Fermi liquid parameter and P_S is the total density of states. As mentioned earlier, neither this model nor any of the other existing models can be considered definitive at this point.

Fig. 6 shows the magnetization loop (top) and temperature dependence of difference between field-cooled and zero field-cooled implantation for 5 at.% Mn samples. The overall magnitude of the magnetization in decreased, although the ordering temperature remains roughly similar to that for the lower Mn concentration.

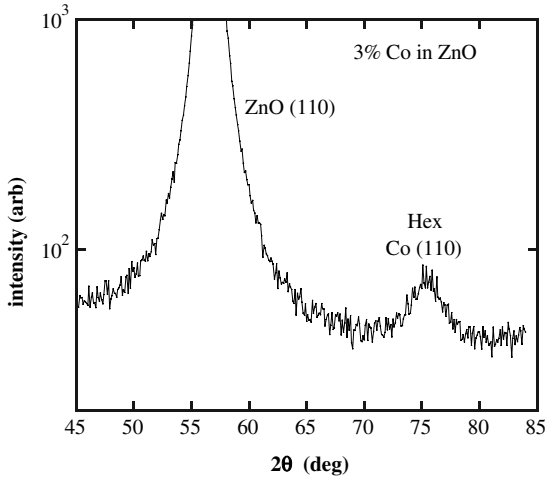

Fig. 4. High resolution XRD spectra from Co-implanted ZnO(5 at.% Co) after annealing at 700 C for 5 min. Peaks due to Co precipitates are clearly visible.

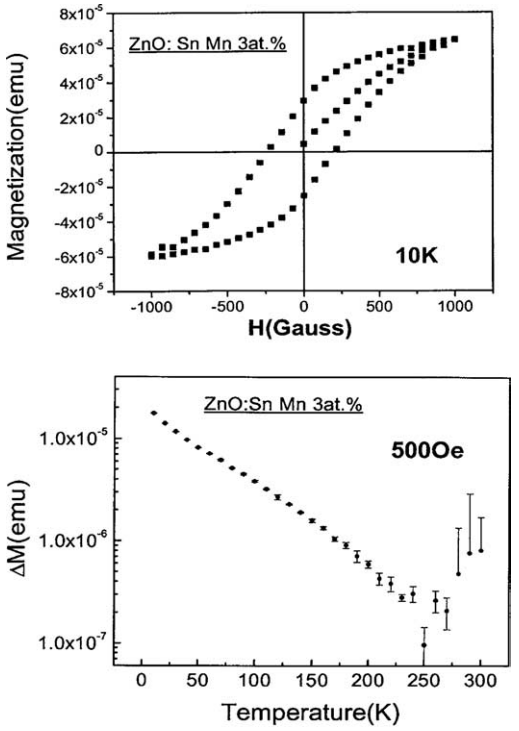

Fig. 5. Magnetization loop at 10 K for field applied perpendicular to the plane of a ZnO sample implanted with 3 at.% Mn (top) and temperature dependence of the difference of field-cooled and zero field-cooled magnetization at a field of 500 Oe (bottom).

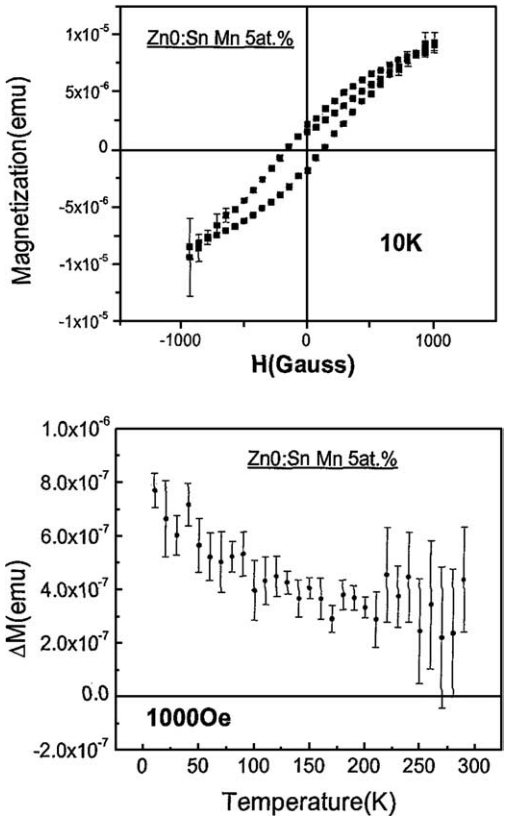

Fig. 6. Magnetization loop at 10 K for field applied perpendicular to the phase of a ZnO sample implanted with 5 at.% Mn (top) and temperature dependence of the difference of field-cooled and zero field-cooled magnetization at a field of 1000 Oe (bottom).

4. Summary and conclusions

Promising magnetic properties were obtained from bulk n-type ZnO crystals directly implanted with Mn or Co at concentrations of 3–4 at.%. Low coercivities (<100 Oe) and high ordering temperatures (250–300 K) were achieved and no second phases were detected in the Mn-implanted material by XRD, however the Co-implanted material show clear evidence of oriented Co precipitates. The origin of the ferromagnetism is still a source of active research and may involve a carrier-induced magnetism, the percolation of magnetic polarons and contributions form precipitates in the Co-implanted material. The M–T curves are non-classical and are consistent with recent disorder models for dilute magnetic semiconductors.

Acknowledgements

The work at UF is partially supported by NSF (DMR-0101856 and DMR-0101438) and by ARO, while the work at SNU is partially supported by KOSEF and Samsung Electronics Endowment through CSCMR.

References

[1] Tiwaii A, Jin C, Kuit A, Kumar D, Muth JF, Narayan J. Solid-State Commun 2002;121:371.
[2] Tang ZK, Yu P, Wong GKL, Kawasaki M, Ohtomo A, Koinuma HH, et al. Solid-State Commun 1997;103:459.
[3] Look DC, Hemsky JW, Sizelove JR. Phys Rev Lett 1999;82:2552.
[4] Minegishi K, Koiwai Y, Kikuchi Y, Yano K, Kasuga M, Shimizu A. Jpn J Appl Phys 1997;36:L1453.
[5] Rouleau C, Kang S, Lowndes D, unpublished.
[6] Yamamoto T, Katayama-Yoshida H. Jpn J Appl Phys 1999;38:L166.
[7] Joseph M, Tabata H, Kawai T. Jpn J Appl Phys 1999; 38:L1205.
[8] Aoki T, Hatanaka Y, Look DC. Appl Phys Lett 2000; 76:3257.
[9] Ryu YR, Zhu S, Look DC, Wrobel JM, Jeong HM, White HW. J Cryst Growth 2000;216:330.
[10] Dietl T, Ohno H, Matsukura F, Cibert J, Ferrand D. Science 2000;287:1019.
[11] Sato K, Katayama-Yoshida H. Jpn J Appl Phys 2001; 40:L334.
[12] Sato K, Katayama-Yoshida H. Jpn J Appl Phys 2000;39:L555.
[13] Sato K, Katayama-Yoshida H. Physica E 2001;10:251.
[14] Sato K, Katayama-Yoshida H. Mater Res Soc Symp Proc 2001;666:F4–6.
[15] Yamamoto T, Katayama-Yoshida H. Jpn J Appl Phys 1999;38:L166.
[16] Fukumura T, Jin Z, Kawasaki M, Shono T, Hasegawa T, Koshikara S, et al. Appl Phys Lett 2001;78:958.
[17] Wakano T, Fujimura N, Morinaga Y, Abe N, Ashida A, Ito T. Physica E 2001;10:260.
[18] Jin Z, Hasegawa K, Fukumura T, Yoo YZ, Hasegawa T, Koinuma H, et al. Physica E 2001;10:256.
[19] Jung SW, An S-J, Yi G-C, Jung CU, Lee S-I, Cho S. Appl Phys Lett 2002;80:4561.
[20] Veda K, Tabota H, Kamai T. Appl Phys Lettt 2001;79:988.
[21] Berciu M, Bhatt RN. Physica B 2002;312/313:815.
[22] Berciu M, Bhatt RD. Phys Rev Lett 2001;87:107203.
[23] Angelescu DE, Bhatt RH. Phys Rev Lett 2002;65:075211.
[24] Durst AC, Bhatt RN, Wolff PA. Phys Rev B 2002; 65:235205.
[25] Bhatt RN, Berciu M, Kennett MD, Wan X. J Supercond: Incorporating Novel Magnetism 2002;15:71.
[26] Lee JS, Khim ZG, Park YD, Norton DP, Theodoropoulou NA, Hebard AF, et al. Solid-State Electron, in press.